Bone Reports 5 (2016) 214–221

Contents lists available at ScienceDirect

Bone Reports

journal homepage: www.elsevier.com/locate/bonr

The F-actin modulator SWAP-70 controls podosome patterning in osteoclasts

Anne Roscher [a], Tomoka Hasegawa [b], Sebastian Dohnke [c], Carlos Ocaña-Morgner [a], Norio Amizuka [b], Rolf Jessberger [a,*,1], Annette I. Garbe [a,c,**,1]

[a] Institute of Physiological Chemistry, Technische Universität Dresden, Germany
[b] Department of Developmental Biology of Hard Tissue, Graduate School of Dental Medicine, Hokkaido University, Sapporo, Japan
[c] Osterimmunology, DFG-Center for Regenerative Therapies, Technische Universität Dresden, Germany

ARTICLE INFO

Article history:
Received 14 April 2016
Accepted 15 July 2016
Available online 19 July 2016

Keywords:
Actin cytoskeleton
Podosome pattering
Membrane binding
PIP3
Swap-70
V-ATPase

ABSTRACT

Osteoclasts are bone resorbing cells acting as key mediators of bone disorders. Upon adhesion to bone, osteoclasts polarize and reorganize their cytoskeleton to generate a ring-like F-actin-rich structure, the sealing zone, wherein the osteoclast's resorptive organelle, the ruffled border, is formed. The dynamic self-organization of actin-rich adhesive structures, the podosomes, from clusters to belts is crucial for osteoclast-mediated bone degradation. Mice lacking the protein SWAP-70 display an osteopetrotic phenotype due to defective bone resorption caused by impaired actin ring formation in *Swap-70*$^{-/-}$ osteoclasts. To further elucidate the mechanisms underlying this defect, we investigated the specific function of SWAP-70 in the organization and dynamics of podosomes. These detailed studies show that the transition from podosome clusters to rings is impaired in *Swap-70*$^{-/-}$ osteoclasts. Live cell imaging of dynamic F-actin turnover and SWAP-70 localization during podosome patterning indicate that SWAP-70 is dispensable for cluster formation but plays a key role in F-actin ring generation. Our data provide insights in the role of SWAP-70's F-actin binding domain and pleckstrin homology (PH) domain in the proper localization of SWAP-70 and formation of a peripheral podosome belt, respectively. *Ex vivo* bone analyses revealed that SWAP-70-deficient osteoclasts exhibit defective ruffled border formation and V-ATPase expression. Our findings suggest an important role of membrane binding of SWAP-70 for the regulation of actin dynamics, which is essential for podosome patterning, and thus for the resorptive activity of osteoclasts.

1. Introduction

Osteoclasts are large multinucleated bone-resorbing cells of hematopoietic origin that develop along the monocyte-macrophage lineage (Arai et al., 1999; Boyle et al., 2003; Udagawa et al., 1990; Walker, 1975a, 1975b). Osteoclast differentiation is regulated by receptor activator of NF-κB ligand (RANKL) and macrophage colony-stimulating factor (M-CSF) binding to their corresponding receptors RANK and c-Fms (Nakagawa et al., 1998; Yasuda et al., 1998; Yoshida et al., 1990). Elevated osteoclast activity leads to osteoporosis, a bone disease characterized by increased, pathological bone loss, while dysfunction or lack of osteoclasts leads to osteopetrosis, a bone disorder characterized by high bone mass (Lazner et al., 1999). The resorptive activity of osteoclasts critically depends on their tight attachment to mineralized matrix and consequent polarization and formation of a convoluted membrane, the so-called ruffled border. To dissolve inorganic hydroxyapatite by acidification of the subjacent lacuna, protons are translocated through the membrane-rich ruffled border by a vacuolar-type H^+-ATPase proton pump (Tolar et al., 2004; Novack and Teitelbaum, 2008; Georgess et al., 2014), while proteolytic enzymes such as Cathepsin K are secreted in order to degrade the organic phase of bone (Blair et al., 1989; Saftig et al., 1998). The ruffled border is surrounded by a F-actin-rich structure, the actin ring or sealing zone, isolating the resorption lacuna from the extracellular space (Novack and Teitelbaum, 2008; Cappariello et al., 2014). The sealing zone forms a large circular band of F-actin lined on both sides by vinculin (Lakkakorpi and Vaananen, 1991; Saltel et al., 2004) and contains densely packed podosomes as adhesive structures. Although podosomes are also present in other highly motile cells such as macrophages or dendritic cells and in smooth muscle cells, endothelial cells and transformed fibroblasts (Gimona et al., 2008), it is only in mature osteoclasts that they dynamically arrange into specialized membrane-proximal ring-like patterns to migrate and to resorb bone.

* Correspondence to: R. Jessberger, Institute of Physiological Chemistry, Technische Universität Dresden, Fiedlerstrasse 42, 01307 Dresden, Germany.
** Correspondence to: A.I. Garbe, Osteoimmunology, DFG-Center for Regenerative Therapies, Technische Universität Dresden, Fetscherstraße 105, 01307 Dresden, Germany.
E-mail addresses: rolf.jessberger@tu-dresden.de (R. Jessberger), Annette.garbe@crt-dresden.de (A.I. Garbe).
[1] Shared senior authorship.

http://dx.doi.org/10.1016/j.bonr.2016.07.002

Podosomes are dot-like structures comprising an F-actin core, which contains various actin polymerization regulator proteins and a surrounding F-actin cloud, a loose network of radial F-actin cables associated with integrins, vinculin, paxillin and talin, and other proteins such as different kinases. During the early stages of osteoclast differentiation, podosomes are organized in clusters, which assemble into

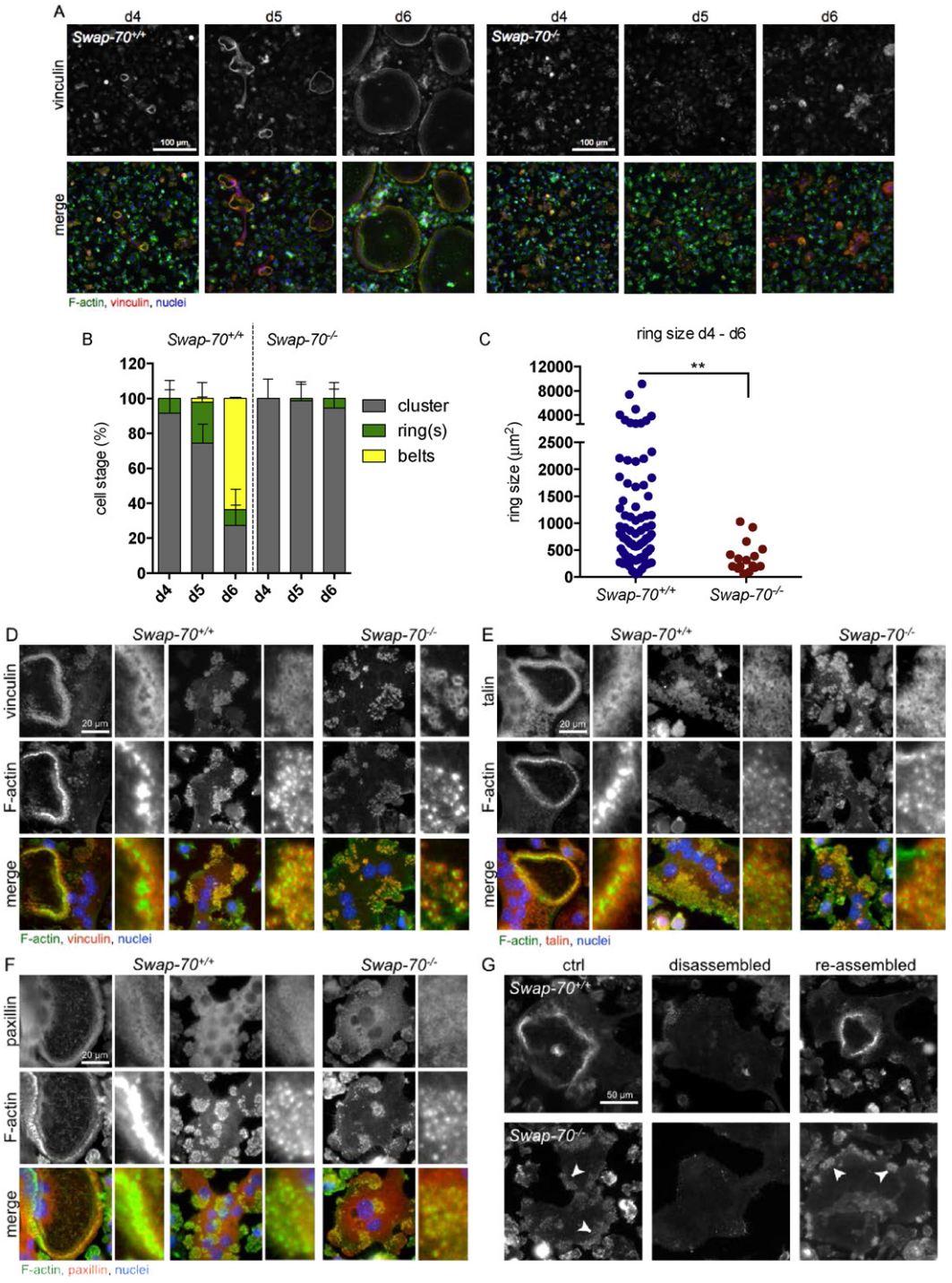

Fig. 1. *Swap-70*$^{-/-}$ BMOCs are impaired in podosome dynamics but not in assembly of podosomes. (A) Immunofluorescence staining of podosomes (vinculin, red; F-actin, green; nuclei, blue) from wild-type (left) and *Swap-70*$^{-/-}$ (right) BMOCs at day 4, day 5 and day 6 of *in vitro* culture. (B) Quantification of BMOCs containing podosome clusters (grey), rings (green) or belts (yellow) as assessed in (A) at day 4, day 5 and day 6. For quantification five fields of view per sample (day 4: 3 slides, day 5: 3 slides, day 6: 4 slides per genotype) were used as assessed in (A). All values are presented as mean ± standard deviation. (C) Size of F-actin rings in wild-type BMOCs and *Swap-70*$^{-/-}$ BMOCs (d4 to d6, five fields of view of 11 slides in total) as assessed in (A). (D–F) Immunofluorescence staining of podosome-associated proteins (D) vinculin (vinculin, red; F-actin, green; nuclei, blue), (E) talin (talin, red; F-actin, green; nuclei, blue), (F) paxillin (paxillin, red; F-actin, green; nuclei, blue) from *Swap-70*$^{+/+}$ and *Swap-70*$^{-/-}$ BMOCs at day 4 or day 5 of *in vitro* culture. The two sets of images arranged in columns in Fig. 1D–F display the different patterns of podosome organization in *Swap-70*$^{+/+}$ osteoclasts (columns 1–4, from left to right), *i.e.* ring (columns 1 and 2) and cluster (columns 3 and 4) formation, and cluster formation (columns 5 and 6) in *Swap-70*$^{-/-}$ osteoclasts. The small pictures in columns 2, 4 and 6 of each figure represent detail enlargements of the actin cores surrounded by vinculin (D), talin (E) und paxillin (F), respectively. (G) F-actin ring reformation assay was performed as described by Kim et al. (2006). F-actin was visualized with Phallodin-Alexa Fluor 488. Left: cells before podosome disassembly (ctrl), middle: cells after treatment with serum-free medium (disassembled) and right: cells after RANKL-induced re-assembly of F-actin rings and podosome clusters (re-assembled). All experiments were performed in 2–3 replicates.

dynamic short-lived F-actin rings with a half-life of several minutes, while mature osteoclasts exhibit podosome belts at the cell periphery (Georgess et al., 2014; Luxenburg et al., 2007; Destaing et al., 2003). These osteoclast-specific superstructures are essential for osteoclasts to perform their function. The regulatory mechanisms of the dynamic organization of podosomes in osteoclasts, especially how F-actin rings evolve from podosome clusters are central to understanding bone degradation in health and disease.

The switch-associated protein SWAP-70 carries an unusual arrangement of protein domains and motifs with high amino acid sequence homology to only one other protein, Def-6 (Gupta et al., 2003). A pleckstrin homology (PH) domain in the center of SWAP-70 binds PIP3, the second messenger product generated by PI3K, and mediates membrane localization of the protein (Shinohara et al., 2002; Wakamatsu et al., 2006). Binding of PIP3 is necessary for SWAP-70 to localize to dynamic membrane F-actin structures such as membrane ruffles (Shinohara et al., 2002; Ihara et al., 2004). The C-terminal actin binding domain of SWAP-70 is affiliated with high affinity binding to non-muscle F-actin (Ihara et al., 2006). Between its PH domain and the actin binding domain three coiled-coil regions are located where SWAP-70 oligomerizes *via* a Q/E rich stretch proposed to be necessary for F-actin bundling (Chacon-Martinez et al., 2013). SWAP-70 is expressed in various hematopoietic cells and acts in processes such as F-actin rearrangement, cell morphogenesis, migration, integrin-mediated adhesion, and homing (Borggrefe et al., 1999; Chopin et al., 2010; Ocana-Morgner et al., 2009; Pearce et al., 2006; Sivalenka and Jessberger, 2004; Garbe et al., 2012). SWAP-70-deficiency results in osteopetrosis caused by decreased resorptive activity of osteoclasts failing to form large F-actin rings (Garbe et al., 2012). Thus, SWAP-70 appears to play an important role in the dynamics and organization of F-actin in podosomes. Osteoclasts provide an excellent cellular model to understand the specific function of SWAP-70 in dynamic organization of the actin cytoskeleton. To further elucidate the mechanisms underlying the defective F-actin ring formation in SWAP-70-deficient osteoclasts, in the present study, we investigated SWAP-70 localization and function in podosome organization and actin dynamics. Together, our results demonstrate that structure and assembly of podosome clusters is not affected by SWAP-70-deficiency and indicate that both, the PH and the F-actin binding domain, are required for proper function of primary osteoclasts, and thus identify SWAP-70 as an essential regulator of dynamic self-organization of podosomes into peripheral belts.

2. Materials and methods

2.1. Mice

Swap-70$^{-/-}$ mice have been described previously (Borggrefe et al., 2001). C57BL/6 mice were purchased from Janvier. Mice were housed and bred in the Experimental Center of the Medizinisch-Theoretisches Zentrum (Technische Universität Dresden, Germany) under specific pathogen-free conditions. Animal experiments were performed as approved by the Regierungspräsidium Dresden.

2.2. In vitro generation of bone marrow-derived osteoclasts

Primary bone marrow-derived osteoclasts were generated as described previously (Garbe et al., 2012). Briefly, primary bone marrow-derived monocytes (BMMs) were isolated from the long bones of 8- to 12-week-old mice. For osteoclastogenic differentiation 1×10^6 BMMs/well were cultured on glass cover slips (12 mm diameter, Sarstedt) in 24 well plates using a-MEM complete (a-MEM (Biochrom) containing 20% FCS, 2 mM glutamine, 100 U/mL penicillin and 100 μg/mL streptomycin (Invitrogen)) supplemented with L929-M-CSF-conditioned medium and 40 ng/mL human soluble RANKL produced by *Pichia pastoris* (kindly provided by Bernard Hoflack, Biotec, Technische Universität Dresden, Germany).

2.3. Retroviral transduction

Retrovirus was produced by co-transfecting ecotropic packaging plasmids with GFP-tagged Actin, SWAP-70, mutant SWAP-70-563 or SWAP-70-PHM pMSC retrovirus vectors in 293T cells using Polyethyleneimine (Sigma-Aldrich) as described previously (Garbe et al., 2012). Briefly, BMMs were cultured in the presence of 4% L929-M-CSF-conditioned medium for 48 h on glass slides or osteoblast-derived matrix, followed by infection with virus-containing supernatants for 6 h. After inoculation, cells were cultured under osteoclastogenic conditions in the presence of L929-M-CSF-conditioned medium and RANKL as described.

2.4. Immunocytochemistry

After differentiation on glass cover slips, bone marrow-derived osteoclasts (BMOCs) were stained by immunocytochemistry as described previously (Garbe et al., 2012). For vinculin, talin or paxillin, cells were stained with monoclonal mouse-antibodies (Sigma-Aldrich) and secondary anti-mouse-IgG1-Cy3 (Jackson). A polyclonal rabbit anti-SWAP-70 antibody, produced in our lab and detected using a Cy3-conjugated goat-anti-rabbit antibody (Jackson), was used to assess SWAP-70 expression. Alexa Fluor 488 Phalloidin (Invitrogen) was used to detect F-actin and 4′,6-diamidino-2-phenylindol (DAPI, Roche) for nuclei staining. Samples were mounted with Fluoromount-G (Southern Biotech) and subjected to fluorescent microscopy (Axiophot, Carl Zeiss; Axiovision Software) or confocal microscopy (TCS SP5, Leica).

2.5. F-actin ring reformation assay

F-actin ring reformation was performed as described (Kim et al., 2006) with slight modifications. Primary bone marrow-derived monocyte were isolated from the long bones of 8- to 12-week-old mice and cultured as described above for five days. In order to disassemble podosomes, cells were washed once in cold PBS and starved for 30 min in serum- and cytokine-free a-MEM (Biochrom) at 37 °C and 5% CO_2 in a humidified incubator. Re-assembly of podosomes was induced with fresh a-MEM complete and 40 ng/mL RANKL for 5 h at 37 °C and 5% CO_2 in a humidified incubator. Samples were immediately fixed with 3.7% formaldehyde in PBS and permeabilized with 0.1% Triton X-100 in PBS. Alexa Fluor 488 Phalloidin (Invitrogen) was used to detect F-actin and 4′,6-diamidino-2-phenylindol (DAPI, Roche) to stain nuclei. As controls samples before disassembly and after disassembly were used.

2.6. Live cell imaging

BMMs were transduced with Actin-GFP, SWAP-70-GFP, mutant SWAP-70 563-GFP or PHM-GFP retrovirus as described above. After inoculation with virus, cells were cultured in a-MEM complete supplemented with L929-M-CSF-conditioned medium and RANKL for 30 min, detached by Trypsin/EDTA, transferred to a MatTek 24 multiwell plate (MatTek) and subjected to osteoclast differentiation as described above. Generation of osteoclasts after transduction with SWAP-70 mutants or controls was monitored by confocal microscopy and after transduction with Actin-GFP by fluorescent microcopy (Nikon). For live cell imaging Leibowitz L15 medium (Invitrogen) containing 20% FCS, 2 mM glutamine (Invitrogen), 100 U/mL penicillin and 100 μg/mL streptomycin (Invitrogen) supplemented with L929-M-CSF-conditioned medium and 40 ng/mL RANKL was used.

2.7. FRAP analysis

BMMs were transduced with Actin-GFP retrovirus as described above. Fluorescent recovery after photobleaching (FRAP) analysis was performed at an inverted LeicaTCS SP5 confocal microscope at 37 °C

using the FRAP Wizard as described by Götz and Jessberger (2013) with slight modifications. Each experiment was performed at 70% laser power. 3 images were taken before bleach (pre-bleach) with acousto-optic tunable filter (AOTF) set to 3%, 1 bleaching image with AOTF at 100% with zoom-in and 300 images of fluorescence recovery with AOTF at 3%. The time between frames was minimized (0.096 s/frame). The fluorescence recovery half-time, $t_{1/2}$ was calculated as the time necessary for the fluorescence signal to recover to 50% of the asymptote intensity.

2.8. Transmission electron microscopic (TEM) analysis

Femora from *wild-type* or *Swap-70*$^{-/-}$ mice were removed and immersed in a mixture of 2% paraformaldehyde and 2.5% glutaraldehyde solution for 24 h at 4 °C after euthanasia. Specimens were post-fixed in 1% osmium tetroxide in 0.1 M cacodylate buffer for 4 h at 4 °C, dehydrated in ascending acetone solutions, and embedded in epoxy resin (Epon 812, Taab, Berkshire, UK). Ultrathin sections were prepared using an ultramicrotome and stained with uranyl acetate and lead citrate for transmission electron microscopy (Hitachi H-7100 Hitachi Co. Ltd., Tokyo, Japan) at 80 kV.

2.9. Histochemistry for tartrate-resistant acid phosphatase (TRAP)/vacuolar H^+-ATPase

After inhibition of endogenous peroxidase activity with 0.3% hydrogen peroxidase in methanol for 30 min, dewaxed paraffin sections were pretreated with 1% bovine serum albumin (BSA; Serologicals Proteins Inc. Kankakee, IL) in PBS (1% BSA-PBS) for 30 min. Sections were then incubated for 2 h at room temperature (RT) with rabbit anti-vacuolar H^+-ATPase (Bioss Inc., Boston, MA) diluted at 1:100 with 1% BSA-PBS. This was followed by incubation with horseradish peroxidase (HRP)-conjugated goat anti-rabbit IgG (DakoCytomation, Glostrup, Denmark). For visualization of all immunoreactions, immune complexes were visualized using 3,3′-diaminobenzidine tetrahydrochloride (Dojindo Laboratories, Kumamoto, Japan). Then, histological slides were rinsed with PBS and incubated in a mixture of 2.5 mg of naphthol AS-BI phosphate (Sigma, St. Louis, MO), 18 mg of red violet LB (Sigma) salt, and 100 mM L (+) tartaric acid (0.76 g) diluted in 30 mL of a 0.1 M sodium acetate buffer (pH 5.0) for 15 min at 37 °C for the detection of enzymatic activity of tartrate-resistant acid phosphatase (TRAP).

2.10. Statistical analysis

Statistical significance of the differences between the ring size of *Swap-70*$^{+/+}$ and *Swap-70*$^{-/-}$ BMOCs was assessed using Prism 6.0 software (GraphPad) and the Wilcoxon matched-pairs signed rank test.

3. Results and discussion

3.1. SWAP-70 controls dynamic podosome patterning but not assembly of podosomes

Swap-70$^{-/-}$ mice are osteopetrotic, their osteoclasts fail in efficient bone resorption, and we observed dispersed F-actin structures that accumulate in more irregular, variable areas of the cells and a lack of organized and defined F-actin rings (Garbe et al., 2012). Based on these observations, we hypothesized that SWAP-70 plays an essential role in the dynamics and organization of actin in podosomes, which is crucial for the generation of distinct F-actin rings in mature osteoclasts. In premature osteoclasts, podosomes are clustered in patches, which assemble during differentiation into F-actin rings and eventually evolve into a large peripheral podosome belt (Destaing et al., 2003). To understand the specific function of SWAP-70 in podosomes, we analyzed the emergence of three distinct patterns of podosome organization, (i) podosome clusters, (ii) expanding F-actin rings and (iii) stable peripheral podosome belts, in *Swap-70*$^{-/-}$ and control *Swap-70*$^{+/+}$ bone marrow-derived osteoclasts (BMOCs) during *in vitro* osteoclast differentiation.

Individual podosomes were defined as F-actin cores surrounded by a vinculin ring. We observed that podosome clusters and individual F-actin rings started to be generated in *Swap-70*$^{+/+}$ BMOCs at day 4

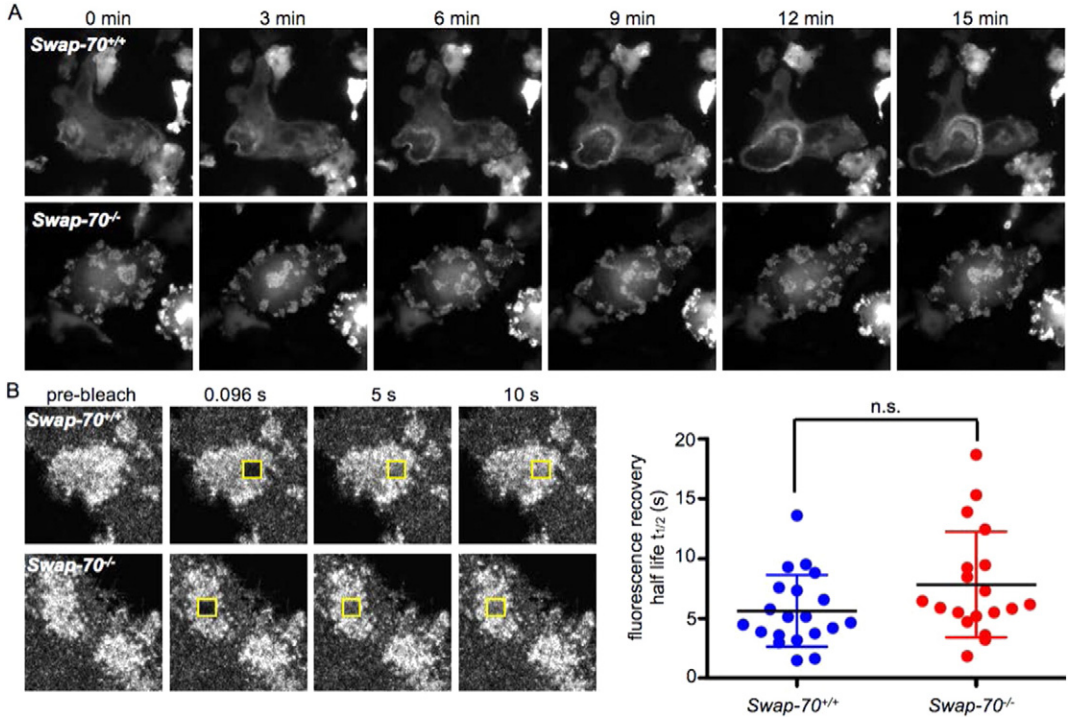

Fig. 2. F-actin turnover in podosome clusters is normal in *Swap-70*$^{-/-}$ BMOCs. (A) Live-cell-imaging of *Swap-70*$^{+/+}$ and *Swap-70*$^{-/-}$ BMOCs 5 days after transduction with actin-GFP. Pictures were taken at indicated time points. (B) FRAP analysis of podosome clusters in *Swap-70*$^{+/+}$ and *Swap-70*$^{-/-}$ BMOCs 5 days after transduction with actin-GFP. Fluorescence recovery half-time, $t_{1/2}$ was calculated as the time necessary for the fluorescence signal to recover to 50% of the asymptote intensity. All experiments were performed in 2–3 replicates.

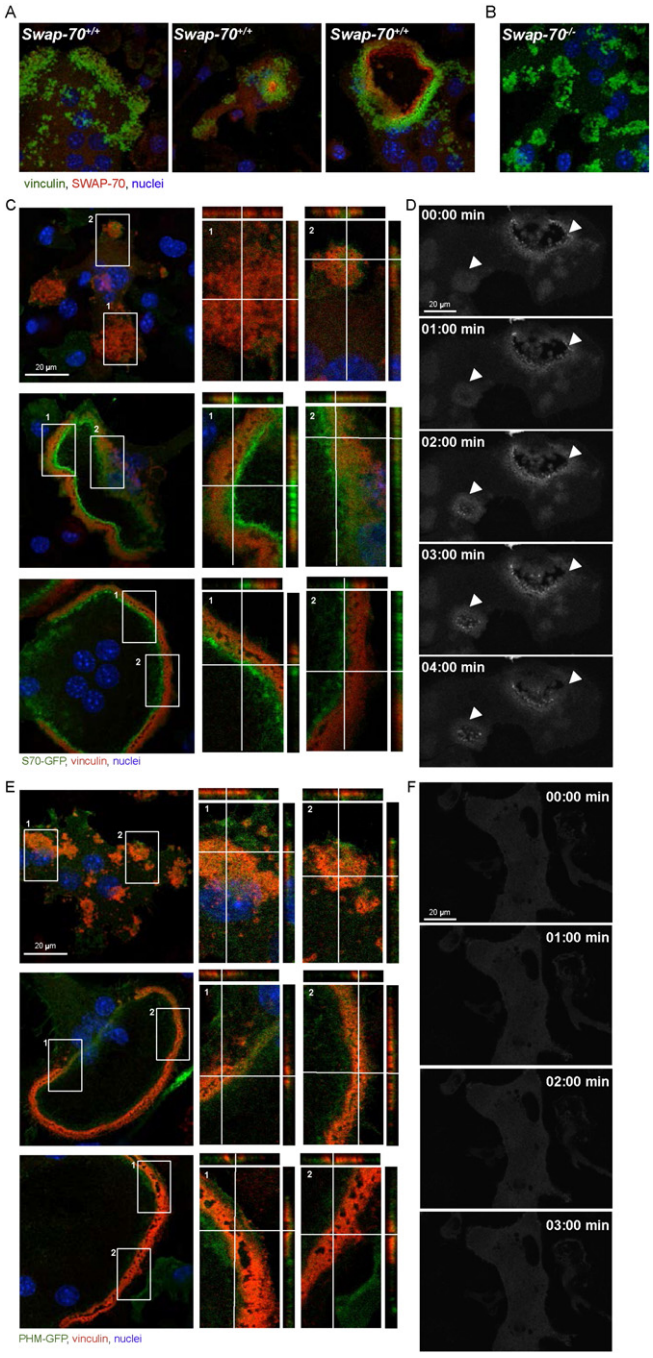

Fig. 3. PIP3 and actin binding are involved in the precise localization of SWAP-70. (A) Immunofluorescence staining of SWAP-70 and vinculin in wild-type BMOCs analyzed by confocal microscopy (SWAP-70, red; vinculin, green; nuclei, blue). (B) *Swap-70*$^{-/-}$ control. (C) Immunofluorescence staining of vinculin in wild-type BMOCs expressing SWAP-70-GFP analyzed by confocal microscopy. Z-stacks of 250 nm size were taken and orthogonal views are shown to further elucidate localization of SWAP-70 in relation to vinculin (vinculin, red; SWAP-70-GFP, green; nuclei, blue). (D) Live-cell-imaging of SWAP-70-GFP 5 days after transduction. Pictures were taken at indicated time points. (E + G) Immunofluorescence staining of vinculin in wild-type BMOCs expressing SWAP-70 mutants, PHM-GFP (E) and SW563-GFP (G), analyzed by confocal microscopy. Z-stacks of 250 nm size were taken and orthogonal views are shown to further elucidate localization of SWAP-70-GFP mutants in relation to vinculin (vinculin, red; PHM-GFP or SW563-GFP, green; nuclei, blue). (F + H) Live-cell-imaging of PHM-GFP (F) and SW563-GFP (H) 5 days after transduction. Pictures were taken at indicated time points. All experiments were performed in 2–3 replicates.

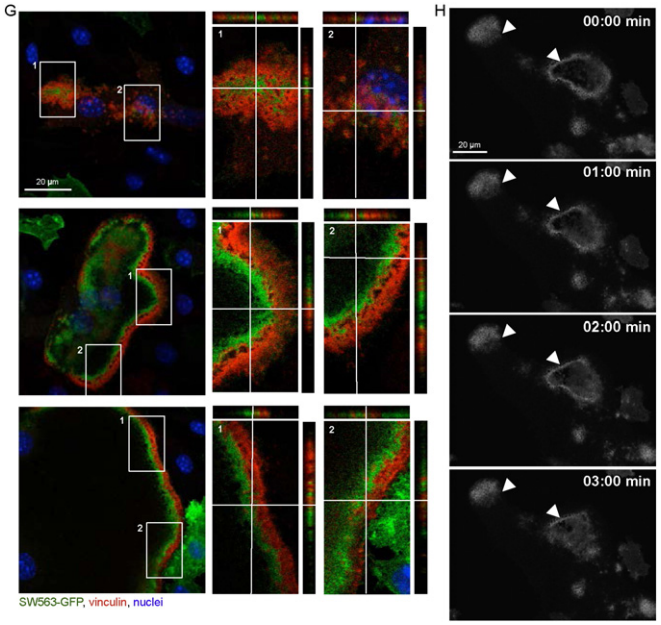

Fig. 3 (*continued*).

and increased in numbers and size at day 5 (Fig. 1A, B). In the absence of SWAP-70, osteoclasts formed podosome clusters at day 4, but very rarely formed individual rings. These were of much smaller average area than those of *Swap-70*$^{+/+}$ BMOCs at days 5 and 6 (Fig. 1A–C). After 6 days of *in vitro* differentiation, when podosomes of *Swap-70*$^{+/+}$ BMOCs had already formed large peripheral podosome belts, the vast majority of *Swap-70*$^{-/-}$ podosomes was still organized in clusters (Fig. 1A, B). These data indicate, that podosomes in *Swap-70*$^{-/-}$ osteoclasts failed to develop beyond the cluster stage and suggest a role for SWAP-70 in the formation and/or stability of the podosome belt.

As shown in Fig. 1A, *Swap-70*$^{-/-}$ podosomes exhibited the typical F-actin cores surrounded by vinculin, suggesting that the basic structure of individual podosomes is not compromised in the absence of SWAP-70. To confirm this assumption, we determined the presence and localization of other adaptor proteins such as talin and paxillin that colocalized with the actin cloud. Like vinculin, talin and paxillin were also localized around F-actin cores in both *Swap-70*$^{+/+}$ and *Swap-70*$^{-/-}$ BMOCs and the size of the cloud appeared also appeared similar (Fig. 1D–F). To more precisely define the impact of SWAP-70 on podosomes and F-actin ring dynamics and to address whether once established F-actin rings or individual podosomes could be rearranged upon disassembly in *Swap-70*$^{+/+}$ or *Swap-70*$^{-/-}$ BMOCs we determined the kinetics of these structures by performing a F-actin ring reformation assay according to Kim et al. (2006). The cells were cultured with M-SCF and RANKL for 5 days, resulting in the formation of osteoclasts with F-actin rings in *Swap-70*$^{+/+}$ but only formation of podosome clusters in *Swap-70*$^{-/-}$ BMOCs (Fig. 1G left). After F-actin ring disruption (Fig. 1G middle) by washing the cells with cold PBS, the cells were incubated in serum- and cytokine-free medium at 37 °C followed by incubation with RANKL, which normally promotes efficient restoration of F-actin ring structures and podosomes (Fig. 1G right). Analysis of this synchronized reformation of actin-rich structures revealed that podosomes in *Swap-70*$^{-/-}$ BMOCs were reformed as fast as in *Swap-70*$^{+/+}$ BMOCs, but no enhanced F-actin ring formation could be observed in this dynamic assay (Fig. 1G bottom), suggesting a regulatory function of SWAP-70 in F-actin ring generation but not in structural assembly of individual podosomes. These findings are in line with our earlier observation that podosome dynamics in dendritic cells does not depend on SWAP-70 (35), and further emphasize a restricted regulatory function of SWAP-70 in expanding F-actin rings in osteoclasts.

3.2. Efficient F-actin turnover in Swap-70$^{-/-}$ podosome clusters

To study live actin dynamics, *Swap-70*$^{+/+}$ and *Swap-70*$^{-/-}$ BMOCs were transduced with actin-GFP retrovirus and subjected to live-cell imaging. As shown in Fig. 2A and in Supplemental movies 1 and 2, podosomes visualized by actin-GFP in *Swap-70*$^{-/-}$ BMOCs were as dynamic and had the same life span as podosomes in *Swap-70*$^{+/+}$ BMOCs. The F-actin turnover within podosomes was studied by Fluorescence recovery after photobleaching (FRAP) in regions of podosome clusters of osteoclasts derived from actin-GFP *Swap-70*$^{+/+}$ and *Swap-70*$^{-/-}$ BMMs. In these FRAP experiments, fluorescence recovery due to actin turnover occurred uniformly throughout the bleached regions in podosome clusters of both, *Swap-70*$^{+/+}$ and *Swap-70*$^{-/-}$ BMOCs (Fig. 2B). Together with the adequate localization of podosomal adaptor proteins, the actin incorporation into *Swap-70*$^{-/-}$ podosomes after photobleaching illustrates that these structures are *bona fide* podosomes.

3.3. PIP3 and F-actin binding are required for proper subcellular localization of SWAP-70

Since our data suggest a function of SWAP-70 in the formation and/or stability of the peripheral podosome belt, we next examined the subcellular distribution of SWAP-70 in premature and mature wild-type osteoclasts. Differentiating osteoclasts with clusters of podosomes and mature osteoclasts with a podosome belt were analyzed by confocal microscopy. In premature osteoclasts, SWAP-70 was localized rather dispersed at podosome clusters (Fig. 3A left; B, negative control: *Swap-70*$^{-/-}$ BMOCs), while the reorganization of the actin cytoskeleton upon osteoclast maturation, which results in the formation of F-actin rings, coincided with a predominant localization of SWAP-70 at the inner side of individual F-actin rings, in close proximity to vinculin (Fig. 3A right). Furthermore, SWAP-70 accumulated at sites where the F-actin ring is just being formed (Figs. 3A middle). To further corroborate these observations, we performed in this study experiments using wild-type BMOCs transduced with SWAP-70-GFP fusion protein. For this purpose, SWAP-70-GFP expressing wild-type osteoclasts were analyzed 5 days after transduction by confocal microscopy and live-cell imaging. These experiments confirmed on the one hand the close association of SWAP-70 with vinculin within podosome clusters and rings and on the other hand clearly demonstrate that SWAP-70 accumulated in BMOCs, then expanded in a ring-like structure and finally dissolved again (Fig. 3C, D and Supplemental movie 3). The differential location of SWAP-70 during the reversible transition between podosome clusters and the podosome belt reflects the important role of SWAP-70 in podosome dynamics.

Our data showed, that a functional PH domain of SWAP-70 is essential for F-actin ring formation and osteoclast function, whereas the deletion of amino acids 564 to 585 of the actin-binding domain located at the very C-terminus of SWAP-70 appears to be dispensable (Shinohara et al., 2002; Garbe et al., 2012). To determine the contribution of these domains to the subcellular distribution of SWAP-70, in the present study, we analyzed the localization of these mutant forms of SWAP-70 by confocal microscopy and live-cell imaging using GFP fusion proteins. These analyses revealed, that PHM-GFP, harboring a non-functional PH domain, was distributed in a dispersed manner in *Swap-70*$^{+/+}$ BMOCs and failed to co-localize with F-actin structures (Figs. 3E, F and Supplemental movie 4). This corroborates our published data, which demonstrated by using IRES-GFP constructs that a functional PH domain of SWAP-70 is essential for F-actin ring formation and bone resorption (Garbe et al., 2012). Furthermore, our localization studies revealed that, in contrast to full-length SWAP-70, SW563-GFP, lacking C-terminal amino acids 564 to 585 of the actin-binding domain (i) accumulated within podosome clusters at vinculin-negative sites (Fig. 3G top) and (ii) was not uniformly aligned in close proximity to vinculin in F-actin rings but more diffusely distributed (Fig. 3G middle and bottom, H and Supplemental movie 5). Still, SW563-GFP associated with the cytoplasmic membrane, supposedly binds PIP3, and thus becomes activated.

We thus propose that a functional PH domain is essential for the recruitment of SWAP-70 to the cell membrane to initiate and support F-actin ring formation. Since during osteoclast activation, the part of the plasma membrane enclosed by the actin ring enlarges into the highly convoluted ruffled border, we furthermore propose an association of SWAP-70 with the ruffled border.

3.4. SWAP-70-deficient osteoclasts are impaired in ruffled border formation

We have previously shown that TRAP-positive osteoclasts are present in osteopetrotic *Swap-70*$^{-/-}$ mice in increased numbers, suggesting that the high bone mass phenotype results from reduced bone degradation by mature cells and not from arrested osteoclastogenesis or increased cell death *in vivo* (Garbe et al., 2012). Therefore, we asked, whether these TRAP-positive *Swap-70*$^{-/-}$ osteoclasts are lacking specific resorptive features such as the ruffled border or vacuolar-type H^+-ATPase, crucial for the ability of osteoclasts to degrade bone. Transmission electron microscopy (TEM) analyses of the tibia and femur of groups of mice showed that in contrast to *Swap-70*$^{+/+}$ osteoclasts the vast majority of SWAP-70-deficient osteoclasts did not exhibit a ruffled border (Fig. 4A), but showed clear zones, important for their ability to seal the resorptive compartment (Teti et al., 1991; Vaananen and Horton, 1995). Further *ex vivo* bone analyses revealed that the majority of *Swap-70*$^{-/-}$ TRAP-positive osteoclasts in the metaphysis lack H^+-ATPase activity (Fig. 4B and Suppl. Fig. 1). These findings are in accordance with the mis-localization of late endosomal and lysosomal glycoprotein LAMP-1, usually located within actin rings (Maeda et al., 1999; Palokangas et al., 1997), in *Swap-70*$^{-/-}$ osteoclasts (Garbe et al., 2012). Absence of ruffled border but presence of clear zones is also described for osteoclasts treated with the vacuolar-type H^+-ATPase inhibitor Bafilomycin indicating a defect in secretion of protons but not in attachment to bone (Sahara et al., 2003). The presence of clear zones in SWAP-70-deficient osteoclasts suggests a defect in properties for effective resorption such as proton secretion through a ruffled border but not attachment to bone (Vaananen and Horton, 1995). F-actin rings surround the so-called ruffled border of osteoclasts important for secretion of hydrochloric acid and proteases. As membrane interaction of SWAP-70 is indispensable for F-actin ring formation, we propose that SWAP-70 serves as a membrane anchor to link the ruffled border to the F-actin ring. Although the actin-binding domain may not be essential to establish the connection of ruffled border and F-actin ring, it may improve the tight association of the two components to maintain best membrane integrity and thereby resorptive function.

In summary, our data show that, while SWAP-70 is dispensable for podosome cluster formation, it controls podosome patterning and ruffled border formation in osteoclasts involving F-actin dynamics after binding to PIP3 in the cell membrane and provide the basis for developing novel strategies for targeting osteoclast activity to combat skeletal disorders.

Supplementary data to this article can be found online at http://dx.doi.org/10.1016/j.bonr.2016.07.002.

Funding information

This work was supported by the Deutsche Forschungsgemeinschaft (DFG, German Research Foundation) through grants JE 150/12-1 and GA1576/1-1/2 (SPP1468 IMMUNOBONE) to RJ and AIG and by the FZT 111 (DFG-Center for Regenerative Therapies Dresden, Cluster of Excellence) to AIG, and three intramural grants from the Technische Universität Dresden (Graduate Academy, MeDDrive Program of the Medical Faculty and Maria Reiche Program) to AR and AIG.

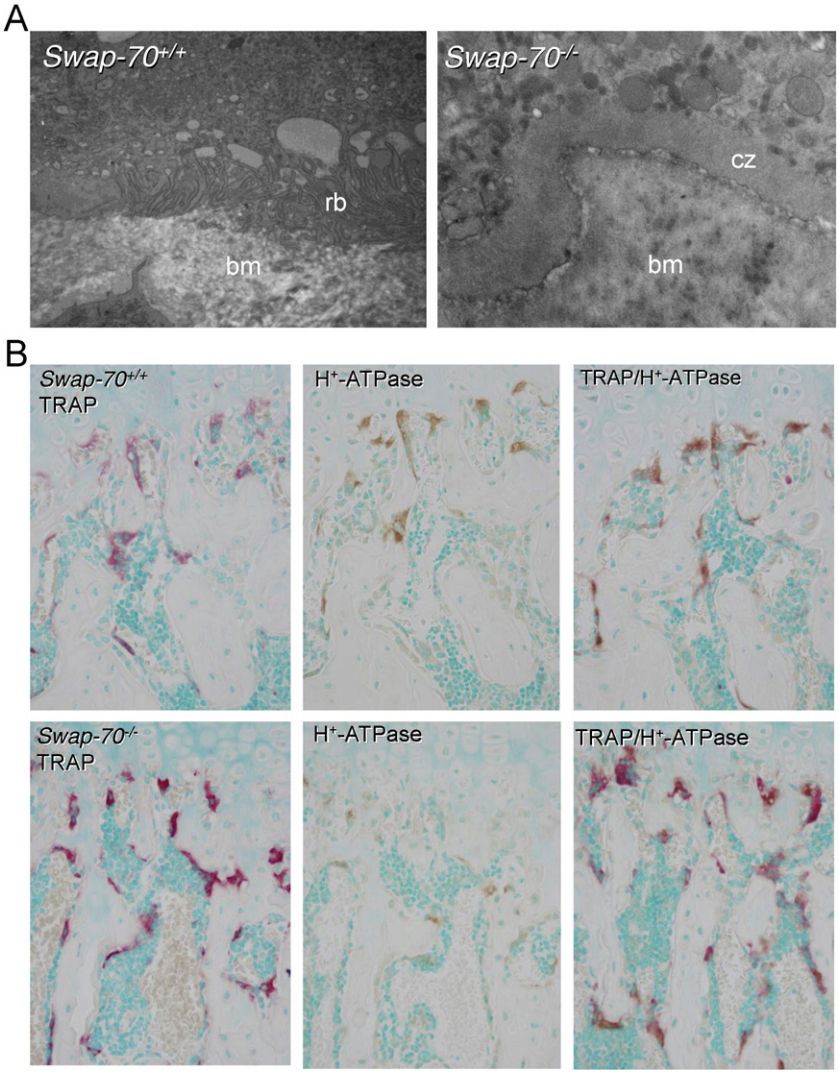

Fig. 4. Impaired ruffled border formation and vacuole-type H^+-ATPase expression in *Swap-70*$^{-/-}$ osteoclasts. (A) Transmission electron microscopy of femoral sections from 11-week-old *Swap-70*$^{+/+}$ (left) and *Swap-70*$^{-/-}$ (right) mice showing representative osteoclasts. Rb: ruffled border, bm: bone matrix, cz: clear zone. (B) Representative images of *Swap-70*$^{+/+}$ (top) and *Swap-70*$^{-/-}$ (bottom) osteoclasts in TRAP (red) and H^+-ATPase (brown) and double-stained decalcified femoral sections. (n = 3 individuals per genotype).

Conflict of interest

The authors declare that there is no conflict of interest.

Acknowledgements

We thank Dirk Lindemann for providing the retroviral expression system, Lorenz Hofbauer for the Paxilin mouse monoclonal antibody, Diana Wehrum and Ute Hempel for resorption plates and Elena Kombarov and Theres Öhler for excellent technical help.

References

Arai, F., Miyamoto, T., Ohneda, O., Inada, T., Sudo, T., Brasel, K., Miyata, T., Anderson, D.M., Suda, T., 1999. Commitment and differentiation of osteoclast precursor cells by the sequential expression of c-Fms and receptor activator of nuclear factor kappaB (RANK) receptors. J. Exp. Med. 190, 1741–1754.

Blair, H.C., Teitelbaum, S.L., Ghiselli, R., Gluck, S., 1989. Osteoclastic bone-resorption by a polarized vacuolar proton pump. Science 245, 855–857.

Borggrefe, T., Masat, L., Wabl, M., Riwar, B., Cattoretti, G., Jessberger, R., 1999. Cellular, intracellular, and developmental expression patterns of murine SWAP-70. Eur. J. Immunol. 29, 1812–1822.

Borggrefe, T., Keshavarzi, S., Gross, B., Wabl, M., Jessberger, R., 2001. Impaired IgE response in SWAP-70-deficient mice. Eur. J. Immunol. 31, 2467–2475.

Boyle, W.J., Simonet, W.S., Lacey, D.L., 2003. Osteoclast differentiation and activation. Nature 423, 337–342.

Cappariello, A., Maurizi, A., Veeriah, V., Teti, A., 2014. The great beauty of the osteoclast. Arch. Biochem. Biophys. 558, 70–78.

Chacon-Martinez, C.A., Kiessling, N., Winterhoff, M., Faix, J., Muller-Reichert, T., Jessberger, R., 2013. The switch-associated protein 70 (SWAP-70) bundles actin filaments and contributes to the regulation of F-actin dynamics. J. Biol. Chem. 288, 28687–28703.

Chopin, M., Quemeneur, L., Ripich, T., Jessberger, R., 2010. SWAP-70 controls formation of the splenic marginal zone through regulating T1B-cell differentiation. Eur. J. Immunol. 40, 3544–3556.

Destaing, O., Saltel, F., Geminard, J.C., Jurdic, P., Bard, F., 2003. Podosomes display actin turnover and dynamic self-organization in osteoclasts expressing actin-green fluorescent protein. Mol. Biol. Cell 14, 407–416.

Garbe, A.I., Roscher, A., Schuler, C., Lutter, A.H., Glosmann, M., Bernhardt, R., Chopin, M., Hempel, U., Hofbauer, L.C., Rammelt, S., Egerbacher, M., Erben, R.G., Jessberger, R., 2012. Regulation of bone mass and osteoclast function depend on the F-actin modulator SWAP-70. J. Bone Miner. Res. 27, 2085–2096.

Georgess, D., Machuca-Gayet, I., Blangy, A., Jurdic, P., 2014. Podosome organization drives osteoclast-mediated bone resorption. Cell Adhes. Migr. 8, 192–204.

Gimona, M., Buccione, R., Courtneidge, S.A., Linder, S., 2008. Assembly and biological role of podosomes and invadopodia. Curr. Opin. Cell Biol. 20, 235–241.

Götz, A., Jessberger, R., 2013. Dendritic cell podosome dynamics does not depend on the F-actin regulator SWAP-70. PLoS One 8.

Gupta, S., Fanzo, J.C., Hu, C.M., Cox, D., Jang, S.Y., Lee, A.E., Greenberg, S., Pernis, A.B., 2003. T cell receptor engagement leads to the recruitment of IBP, a novel guanine nucleotide exchange factor, to the immunological synapse. J. Biol. Chem. 278, 43541–43549.

Ihara, S., Oka, T., Jessberger, R., Fukui, Y., 2004. Involvement of SWAP-70 in membrane ruffling thorough its F-actin binding domain. Mol. Biol. Cell 15, 387A.

Ihara, S., Oka, T., Fukui, Y., 2006. Direct binding of SWAP-70 to non-muscle actin is required for membrane ruffling. J. Cell Sci. 119, 500–507.
Kim, H.J., Zhao, H.B., Kitaura, H., Bhattacharyya, S., Brewer, J.A., Muglia, L.J., Ross, F.P., Teitelbaum, S.L., 2006. Glucocorticoids suppress bone formation via the osteoclast. J. Clin. Investig. 116, 2152–2160.
Lakkakorpi, P.T., Vaananen, H.K., 1991. Kinetics of the osteoclast cytoskeleton during the resorption cycle in vitro. J. Bone Miner. Res. 6, 817–826.
Lazner, F., Gowen, M., Pavasovic, D., Kola, I., 1999. Osteopetrosis and osteoporosis: two sides of the same coin. Hum. Mol. Genet. 8, 1839–1846.
Luxenburg, C., Geblinger, D., Klein, E., Anderson, K., Hanein, D., Geiger, B., Addadi, L., 2007. The architecture of the adhesive apparatus of cultured osteoclasts: from podosome formation to sealing zone assembly. PLoS One 2, e179.
Maeda, H., Akasaki, K., Yoshimine, Y., Akamine, A., Yamamoto, K., 1999. Limited and selective localization of the lysosomal membrane glycoproteins LGP85 and LGP96 in rat osteoclasts. Histochem. Cell Biol. 111, 245–251.
Nakagawa, N., Kinosaki, M., Yamaguchi, K., Shima, N., Yasuda, H., Yano, K., Morinaga, T., Higashio, K., 1998. RANK is the essential signaling receptor for osteoclast differentiation factor in osteoclastogenesis. Biochem. Biophys. Res. Commun. 253, 395–400.
Novack, D.V., Teitelbaum, S.L., 2008. The osteoclast: friend or foe? Annu. Rev. Pathol.: Mech. Dis. 3, 457–484.
Ocana-Morgner, C., Wahren, C., Jessberger, R., 2009. SWAP-70 regulates RhoA/RhoB-dependent MHCII surface localization in dendritic cells. Blood 113, 1474–1482.
Palokangas, H., Mulari, M., Vaananen, H.K., 1997. Endocytic pathway from the basal plasma membrane to the ruffled border membrane in bone-resorbing osteoclasts. J. Cell Sci. 110 (Pt 15), 1767–1780.
Pearce, G., Angeli, V., Randolph, G.J., Junt, T., von Andrian, U., Schnittler, H.J., Jessberger, R., 2006. Signaling protein SWAP-70 is required for efficient B cell homing to lymphoid organs. Nat. Immunol. 7, 827–834.
Saftig, P., Hunziker, E., Wehmeyer, O., Jones, S., Boyde, A., Rommerskirch, W., Moritz, J.D., Schu, P., von Figura, K., 1998. Impaired osteoclastic bone resorption leads to osteopetrosis in cathepsin-K-deficient mice. Proc. Natl. Acad. Sci. U. S. A. 95, 13453–13458.
Sahara, T., Itoh, K., Debari, K., Sasaki, T., 2003. Specific biological functions of vacuolar-type H^+-ATPase and lysosomal cysteine proteinase, cathepsin K, in osteoclasts. Anat. Rec. A Discov. Mol. Cell. Evol. Biol. 270A, 152–161.
Saltel, F., Destaing, O., Bard, F., Eichert, D., Jurdic, P., 2004. Apatite-mediated actin dynamics in resorbing osteoclasts. Mol. Biol. Cell 15, 5231–5241.
Shinohara, M., Terada, Y., Iwamatsu, A., Shinohara, A., Mochizuki, N., Higuchi, M., Gotoh, Y., Ihara, S., Nagata, S., Itoh, H., Fukui, Y., Jessberger, R., 2002. SWAP-70 is a guanine-nucleotide-exchange factor that mediates signalling of membrane ruffling. Nature 416, 759–763.
Sivalenka, R.R., Jessberger, R., 2004. SWAP-70 regulates c-kit-induced mast cell activation, cell-cell adhesion, and migration. Mol. Cell. Biol. 24, 10277–10288.
Teti, A., Marchisio, P.C., Zallone, A.Z., 1991. Clear zone in osteoclast function - role of podosomes in regulation of bone-resorbing activity. Am. J. Phys. 261, C1–C7.
Tolar, J., Teitelbaum, S.L., Orchard, P.J., 2004. Mechanisms of disease: osteopetrosis. N. Engl. J. Med. 351, 2839–2849.
Udagawa, N., Takahashi, N., Akatsu, T., Tanaka, H., Sasaki, T., Nishihara, T., Koga, T., Martin, T.J., Suda, T., 1990. Origin of osteoclasts: mature monocytes and macrophages are capable of differentiating into osteoclasts under a suitable microenvironment prepared by bone marrow-derived stromal cells. Proc. Natl. Acad. Sci. U. S. A. 87, 7260–7264.
Vaananen, H.K., Horton, M., 1995. The osteoclast clear zone is a specialized cell-extracellular matrix adhesion structure. J. Cell Sci. 108, 2729–2732.
Wakamatsu, I., Ihara, S., Fukui, Y., 2006. Mutational analysis on the function of the SWAP-70 PH domain. Mol. Cell. Biochem. 293, 137–145.
Walker, D.G., 1975a. Bone resorption restored in osteopetrotic mice by transplants of normal bone marrow and spleen cells. Science 190, 784–785.
Walker, D.G., 1975b. Spleen cells transmit osteopetrosis in mice. Science 190, 785–787.
Yasuda, H., Shima, N., Nakagawa, N., Yamaguchi, K., Kinosaki, M., Mochizuki, S., Tomoyasu, A., Yano, K., Goto, M., Murakami, A., Tsuda, E., Morinaga, T., Higashio, K., Udagawa, N., Takahashi, N., Suda, T., 1998. Osteoclast differentiation factor is a ligand for osteoprotegerin/osteoclastogenesis-inhibitory factor and is identical to TRANCE/RANKL. Proc. Natl. Acad. Sci. U.S.A. 95, 3597–3602.
Yoshida, H., Hayashi, S., Kunisada, T., Ogawa, M., Nishikawa, S., Okamura, H., Sudo, T., Shultz, L.D., 1990. The murine mutation osteopetrosis is in the coding region of the macrophage colony stimulating factor gene. Nature 345, 442–444.